Color Contrast Induction

BENJAMIN SINGER,* MICHAEL D'ZMURA*

We report the results of psychophysical experiments on the intensive, spatial, temporal and chromatic properties of color contrast induction. Modulating the contrast of an annulus induces an apparent modulation of the color contrast of a central disk, at isoluminance. Results of varying the size of the annulus suggest that mechanisms which control contrast gain are spatially localized. Results of varying the orientations of disk and annulus patterns, with peak spatial frequencies at about 2 c/deg, suggest that the mechanisms are spatially isotropic. Results of varying the rate at which annulus contrast is modulated shows that mechanisms which mediate contrast induction have a low-pass temporal sensitivity that cuts off at about 8 Hz. Results of an experiment on the interocular transfer of color contrast induction suggest that the induction has a cortical locus. Finally, the results of varying the chromatic properties of disk and annulus suggest that the underlying mechanisms are partially, but not fully, chromatically selective.

Color appearance   Color contrast   Color induction   Color constancy

I. INTRODUCTION

Psychophysical experiments have revealed several components in the response of the human visual system to changes in average light levels. These include multiplicative processes that regulate sensitivity in the cone photoreceptoral mechanisms. Hypothesized by von Kries to act independently within each cone class, these processes play a basic role in determining color appearance (von Kries, 1905; Judd, 1940; Worthey & Brill, 1986; D'Zmura & Lennie, 1986; Brainard & Wandell, 1992). There are also second sites of adaptation, which are driven by opposed signals from different classes of cone. These second sites are revealed in experiments with chromatically-extreme background lights, like those using Stiles' two-color increment threshold technique (Stiles, 1949; Pugh & Mollon, 1979). The time–course of their adaptation is thought to be on the order of at least tens of seconds (Augenstein & Pugh, 1977; Loomis, 1980; Fairchild & Lennie, 1992). Third, there are fast-acting lateral inhibitory mechanisms that underlie simultaneous contrast and color induction phenomena (Jameson & Hurvich, 1961; Walraven, 1973; Yund & Armington, 1975; DeValois, Webster, DeValois & Lingelbach, 1986; Krauskopf, Zaidi & Mandler, 1986a). Lateral inhibition can adjust central appearance rapidly in response to changes in the average light from surrounding areas.

The response of the visual system to changes in contrast about some average level has also been investigated psychophysically. Krauskopf *et al.* demonstrated

*Department of Cognitive Sciences & Institute for Mathematical Behavioral Sciences, University of California, Irvine, CA 92717, U.S.A. [*Email* bens@euclid.ss.uci.edu].

habituation to color contrast in studies that showed how viewing slow heterochromatic flicker can cause prolonged desensitization of color-opponent mechanisms (Krauskopf, Williams & Heeley, 1982; Krauskopf, Williams, Mandler & Brown, 1986b). They showed that habituation increases with increasing duration of viewing and with increasing contrast. The mechanisms that are responsible for habituation evidently control the gain on color contrast, albeit with a sluggish time–course.

More recent studies of color appearance have demonstrated a simultaneous effect on appearance at a central location of the variation in color in surrounding areas (McCann, 1989; Brown & MacLeod, 1992; Brown, 1993; Wesner & Shevell, 1992; Jenness & Shevell, 1993; Bäuml, 1994). These studies show that knowledge of the space-averaged chromaticity of lights from surrounding areas is not sufficient to predict the influence of the surround on the color appearance of a central test.

Chubb, Sperling and Solomon (1989) used achromatic dynamic noise stimuli to reveal fast-acting mechanisms for contrast gain control. They showed that increasing the contrast of texture elements in an annular surround immediately decreases the apparent contrast of elements in a central disk, and *vice versa*. This result could not be accounted for by mechanisms that adapt in responses to changes in the average light level, because the space- and time-averaged lights from the dynamic noise stimuli were steady.

We wanted to learn about mechanisms sensitive to color contrast modulations like those revealed by Chubb *et al.* (1989) with achromatic properties. The experiments were designed to document the presence of contrast gain control mechanisms that are sensitive to isoluminant modulations of contrast, and to survey their

basic properties. This work was reported in preliminary form elsewhere (Singer & D'Zmura, 1992; Singer, Han & D'Zmura, 1993).

II. METHODS

Stimuli were presented on a Sony Trinitron GDM-1960 color monitor that observers viewed binocularly at a distance of 1 m in a dark room. Software on a DECstation 5000/200 controlled a Turbo PXG + color graphics board that was set to provide eight bits of chromatic information for each of the 1280 × 1024 pixels presented on the monitor at a field rate of 66 Hz (non-interlaced). The nonlinear relationship between applied voltage and phosphor intensity was corrected, for each gun, using eight-bit color lookup tales. The spectra, chromaticities and luminances of the three EBU phosphors of the monitor were measured using a Photo Research PR-650 SpectraColorimeter. Within the limits of measurement accuracy, the spectra were the same as those reported by Arend and Reeves (1986). The screen was set to display a steady, neutral background with luminance 51.5 cd/m² and a chromaticity (0.285,0.300) for the CIE 1931 standard observer.

We used a 512 × 512 pixel disk-annulus configuration for the binary spatial noise patterns that were presented to the observers (see Fig. 1). The radii of the disk and annulus were 1 and 4 deg of visual angle, respectively. A binary noise pattern was computed by (1) specifying a spatially-isotropic difference of Gaussians amplitude spectrum, where the two Gaussians had identical peak values and had spatial standard deviations of 0.625 and
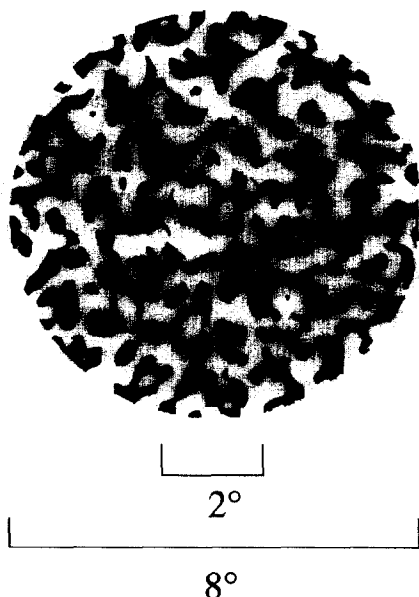

FIGURE 1. Stimulus spatial properties. A central disk of radius 1 deg visual angle and an annulus with an outer radius of 4 deg visual angle were filled with binary spatial noise. The stimulus was centered on a gray rectangular background, 20 deg wide × 16 deg high. The peak spatial frequency of the noise was estimated to be, on average, 1.8 c/deg, found by estimating the average number of zero-crossings along diameters of binary noise disks of radius 4 deg.
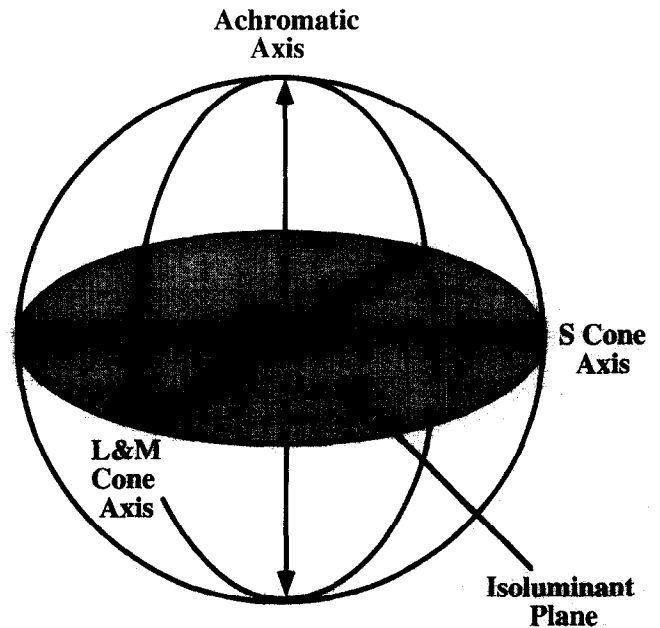

FIGURE 2. Color space. The L & M cone axis and the S cone axis pass through the white point W and span the isoluminant plane, modulations within which are invisible to a mechanisms with the V_λ photopic spectral sensitivity. An achromatic axis completes the space.

1.875 deg of visual angle; (2) generating a random phase spectrum; (3) applying an inverse Fourier transform to the amplitude and phase spectra to produce spatial noise; and (4) binarizing the result to produce binary spatially-isotropic noise with peak energy in its spatial frequency spectrum at about 1.8 c/deg.

The chromatic properties of the disk and the annulus were modulated independently by color lookup table animation. We describe these chromatic properties in the color space of Krauskopf and colleagues (MacLeod & Boynton, 1979; Krauskopf et al., 1982; Derrington, Krauskopf & Lennie, 1984). As depicted in Fig. 2, an isoluminant plane passes through a point W that represents the neutral background of intermediate intensity to which the observers remain adapted. The isoluminant plane, which we define by photometric measurement, is spanned by two axes: (1) the L & M cone axis, modulations along which are visible only to the long-wavelength-sensitive L cones and the medium-wavelength-sensitive M cones, and (2) the S cone axis, modulations along which are visible only to the short-wavelength-sensitive S cones. We use the Smith and Pokorny (1975) fundamentals to determine these axes. Saturated lights along the L & M cone axis appear red or blue-green, while lights along the S cone axis appear yellow-green or purple. An achromatic axis, along which intensity is modulated to produce lights that appear as various shades of gray, completes this color space. Calculations using the Smith and Pokorny (1975) fundamentals and measurements using the spectroradiometer show that the maximum contrast available to us along the L & M cone axis was 0.088 contrast to L cones, while the maximum contrast available along the S cone axis was 0.89 to S cones. Because we defined our color space
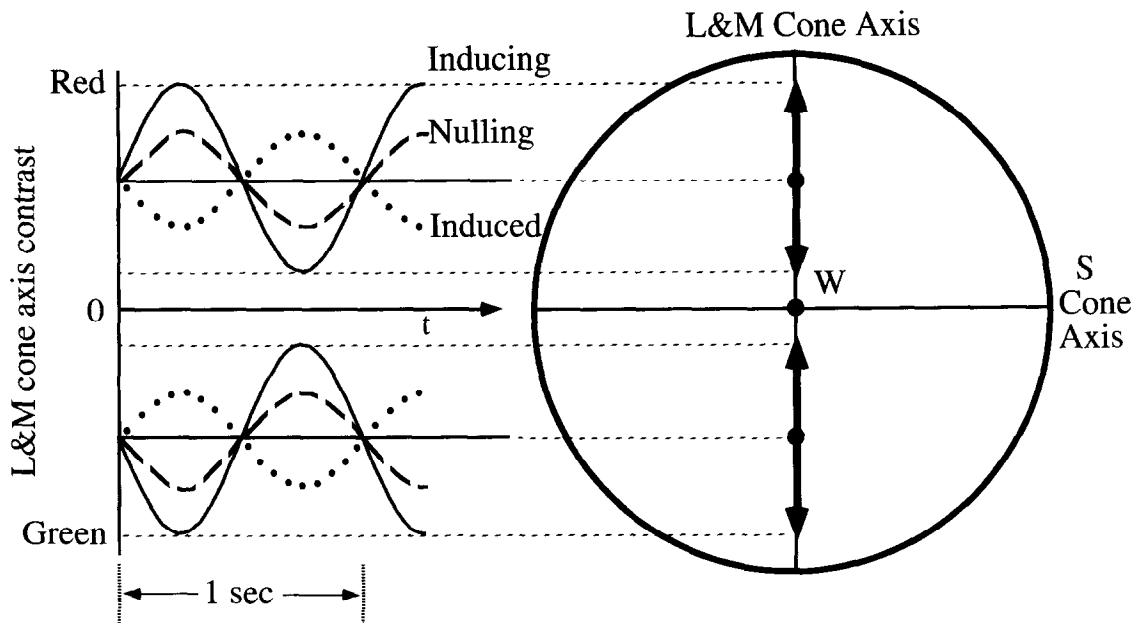
FIGURE 3. Stimulus chromatic properties. On the left is shown the time-varying contrast modulation of an annulus (solid lines, Inducing) with mean contrast and contrast modulation along the L & M cone axis. The dotted lines (Induced) show the induced modulation in the appearance of a physically-steady central disk with L & M cone axis chromaticities. The dashed line (Nulling) depict the physical modulation of the disk that is required to null the fluctuation in appearance, namely to make it appear steady.

axes using the Smith and Pokorny (1975) fundamentals, the true cardinal axes of individual observers might deviate slightly from the axes used, due to individual differences.

Both annulus and disk contained binary noise; consequently each presented two (generally distinct) lights at any one time. We varied the annulus lights to modulate contrast but leave the space-averaged light unchanged. As shown in Fig. 3, the two regions of the annulus were assigned complementary colors along an axis through the white point, with the result that the space-averaged light and the time-averaged light from the annulus were equivalent to the gray background. Figure 3 describes the case where the annulus has red and blue-green regions with chromaticities drawn from the L & M cone axis. The two annulus lights were modulated sinusoidally about their mean values to produce a contrast modulation along a color space axis identical to that along which lay the means. The software let us control the color space axis of the mean values and the modulation, the contrast about the white point provided by the mean values, the amplitude of the contrast modulation and the temporal frequency of the modulation.

We performed a simple test to confirm that annulus contrast could be varied independently of disk physical properties. The spectroradiometer was used to measure the dependence on annulus contrast of the luminance and chromaticity of a uniform, gray disk. Central disk luminances and CIE 1931 (x,y) chromaticities were measured at 10 different annulus contrast values ranging from 10% to 100% of the maximum available contrasts along each of the three cardinal axes. There was no discernible dependence of either disk luminance or disk

chromaticity on annulus contrast. The standard deviations of the ten luminance measurements along each axis represented approx. 0.2% contrast about the disk mean luminance 51.5 cd/m², while the standard deviations of the 10 chromaticity measurements along each axis were <0.001 for both x and y chromaticity values.

In the experiments, the central disk comprised binary noise using lights that possessed complementary chromaticities. When the two lights from the disk were held steady, it was often the case that modulating the contrast of the annulus (Fig. 3, solid curves) induced an apparent contrast modulation of the central disk in counterphase (Fig. 3, dotted curves). Increasing the contrast of an annulus, for instance, often caused an apparent reduction in the contrast of the central disk, while decreasing annulus contrast often caused an apparent increase in disk contrast. At isoluminance, such changes in disk contrast appeared as modulations of color saturation. These observations with static noise patterns recall the results of Krauskopf et al. (1986a) with spatially-uniform fields and the results of Chubb et al. (1989) with dynamic, achromatic noise.

Following Krauskopf et al. (1986a) and Chubb et al. (1989), we modulated the contrast of the disk sinusoidally (Fig. 3, dashed curves) in an attempt to null the induced contrast modulation so that the appearance of the disk remained steady. Potential nulling modulations were always chosen from the set of modulations of disk contrast along the color space axis identical to that along which lay the two disk chromaticities. In Fig. 4, for instance, the nulling modulation is a modulation of contrast along the L & M cone axis. In all experiments but that on chromatic selectivity, annulus and
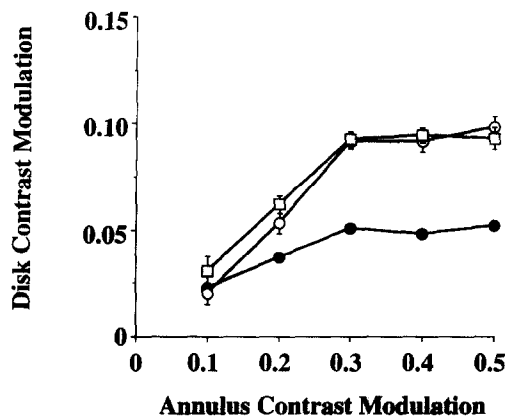
FIGURE 4. Results of varying the amplitude of the annulus contrast modulation. The dependence of nulling contrast modulation on the amplitude of annulus contrast modulation is shown for achromatic stimuli (●), L & M cone axis stimuli (○) and S cone axis stimuli (□). The plotted points represent the average nulling contrast modulations determined for four observers; error bars represent estimates of the SEMs. The mean contrasts of the disks and annuli were fixed at 0.5. The contrasts are expressed in terms of the maximum available along each of the three axes: 1.0 to all cone classes along the achromatic axis, 0.088 to the L cones along the L & M cone axis, and 0.89 to the S cones along the S cone axis. The average nulling contrast modulations for the four observers and the average intervals of uncertainty are listed in Table 1.

disk chromaticities lay along a single axis in any one condition.

The observers' task was to determine the amplitude of nulling modulation that was required to eliminate the apparent change in disk appearance caused by modulating the contrast of the annulus. We used the method of limits. Each experimental run consisted of three ascending and three descending sequences presented in alternation. Each sequence had 11 trials. In descending sequences, the initial disk contrast modulation was chosen to be large and in phase with the annulus modulation—a large positive contrast modulation. On further trials in a descending sequence, the disk contrast modulation decreased steadily to zero. In some conditions the modulation would pass through zero, reverse in phase, and increase again, out of phase with the annulus modulation, so providing negative contrast modulations. The sequence of trials was reversed in ascending sequences.

Observers adapted to the neutral gray, steady background for 1 min at the beginning of each experimental run. Each trial began with two beeps after an interstimulus interval of 1 sec. The disk-annulus stimulus appeared 1 sec later. The observer was instructed to respond as rapidly as possible by pressing one of three keys. These keys indicated whether (1) the central disk contrast appeared to be modulated in phase with the annulus modulation; (2) the appearance of the central disk was steady; or (3) the central disk contrast appeared to be modulated in counterphase to the annulus modulation. The stimulus disappeared immediately after a response. The transition from response type (1) to response type (2) provides an upper threshold, while the transition from response type (2) to response type (3)

provides a lower threshold. The average of lower and upper thresholds, taken across the six sequences, was used to estimate the nulling contrast modulation. The difference between the average upper threshold and the average lower threshold was used to estimate the interval of uncertainty.

Five observers participated in these experiments, including the authors BS and MD and three naive observers LD, KH and JL. JL participated only in the ring distance and chromatic selectivity experiments and in the experiment to control for luminance artifacts. All had normal color vision, as tested using Ishihara plates (Ishihara, 1986), and were properly refracted. Results for the observers were very similar. We present the results using plots of the averages of the observer's nulling contrast modulations; unless otherwise stated, error bars represent estimates of the SEM for the four observers. In Table 1 we present the average nulls and the corresponding intervals of uncertainty, averaged across observers, for each plotted average nulling contrast modulation. Results are scaled according to the maximum contrast available along each axis.

III. RESULTS

Annulus contrast modulation

In a first experiment, we determined the magnitude of induced contrast modulation for annulus contrast modulations along the achromatic, L & M cone, and S cone axes. We were particularly interested in learning the strength of induced contrast modulation along the two isoluminant axes. Are contrast gain control mechanisms sensitive to color contrast?

The mean contrast of the annulus was held fixed at half the maximum available along each of the axes. The strength of the contrast modulation was varied from 0.1 to 0.5. Setting the annulus contrast modulation to 0.5 caused the entire available range of chromaticities along an axis to be used. For each axis, the central disk was chosen to have a color space axis and a contrast matching that of the annulus average.

We expected to find that induced contrast modulation increases as annulus contrast modulation increases. Figure 4 shows that this expectation is met for annuli and disks along the achromatic axis (solid circles), along the L & M cone axis (open circles) and along the S cone axis (open squares). The contrast modulations of the central disk that were needed to null the induced modulation are plotted as a function of annulus contrast modulation.

The nulling contrast modulations along the three axes share the color space axis of the annulus contrast modulation and are presented relative to the maximum contrast available along each axis (see Methods). The peak nulling contrast modulation of about 0.05 along the achromatic axis corresponds to a modulation of disk contrast between 0.45 and 0.55 about the chosen mean of 0.50. The peak nulling contrast modulations of

TABLE 1. Average nulls and the corresponding intervals of uncertainty

Annulus contrast modulation		0.1	0.2	0.3	0.4	0.5	
(Fig. 4)	A	0.023, 0.007	0.037, 0.006	0.051, 0.007	0.049, 0.008	0.052, 0.011	
	L&M	0.020, 0.043	0.053, 0.027	0.092, 0.019	0.092, 0.025	0.098, 0.020	
	S	0.031, 0.036	0.062, 0.011	0.093, 0.010	0.095, 0.009	0.093, 0.009	

Disk mean contrast		0.125	0.25	0.375	0.5	0.625	0.75
(Fig. 5)	A	0.015, 0.008	0.029, 0.004	0.048, 0.005	0.052, 0.007	0.050, 0.006	0.051, 0.008
	L&M	0.007, 0.007	0.038, 0.008	0.095, 0.011	0.110, 0.014	0.115, 0.015	0.105, 0.015
	S	0.016, 0.007	0.040, 0.014	0.077, 0.013	0.089, 0.015	0.103, 0.011	0.132, 0.010

Annulus outer radius		1.1	1.2	1.35	1.5	2	3	4
(Fig. 6)	A	0.009, 0.013	0.013, 0.017	0.024, 0.016	0.022, 0.020	0.033, 0.012	0.042, 0.007	0.048, 0.008
	L&M	0.015, 0.049	0.034, 0.038	0.057, 0.028	0.059, 0.030	0.079, 0.025	0.094, 0.026	0.097, 0.016
	S	0.007, 0.038	0.031, 0.024	0.036, 0.023	0.058, 0.025	0.084, 0.028	0.093, 0.021	0.090, 0.017

Annulus inner radius		1	2	2.65	3.16	3.65
(Fig. 7)	A	0.038, 0.004	0.030, 0.006	0.023, 0.006	0.016, 0.008	0.013, 0.007
	L&M	0.072, 0.011	0.048, 0.026	0.038, 0.022	0.032, 0.026	0.027, 0.024
	S	0.099, 0.010	0.052, 0.017	0.051, 0.021	0.037, 0.029	0.038, 0.029

Annulus pattern orientation		0	30	60	90	120	150
(Fig. 8)	A	0.049, 0.007	0.050, 0.006	0.050, 0.008	0.051, 0.005	0.051, 0.005	0.049, 0.008
	L&M	0.104, 0.018	0.115, 0.018	0.120, 0.019	0.108, 0.021	0.103, 0.019	0.117, 0.021
	S	0.111, 0.018	0.108, 0.022	0.104, 0.021	0.104, 0.016	0.101, 0.024	0.096, 0.021

Annulus temporal frequency		0.25	0.5	1	2	4	8
Nulling amplitude determination							
(Fig. 9)	A	0.056, 0.011	0.056, 0.008	0.047, 0.008	0.038, 0.012	0.030, 0.023	0.015, 0.024
	L&M	0.111, 0.022	0.102, 0.025	0.099, 0.015	0.112, 0.036	0.078, 0.073	−0.021, 0.150
	S	0.113, 0.026	0.124, 0.016	0.104, 0.018	0.108, 0.021	0.072, 0.061	0.008, 0.150
Temporal phase determination							
(Fig. 10)	A			5.35, 49.4	1.58, 52.4	0.667, 57.9	
	L&M			−1.78, 56.2	−6.32, 58.7	−16.17, 68.1	
	S			7.50, 81.0	−0.625, 57.3	−8.42, 70.2	

Interocular transfer		Annulus left, disk right eye	Annulus left, disk left eye
(Fig. 11)	A	0.041, 0.017	0.047, 0.012
	L&M	0.073, 0.034	0.098, 0.046
	S	0.115, 0.041	0.096, 0.034

Annulus cardinal axis		A	L&M	S
(Fig. 12)	A	0.045, 0.004	0.007, 0.008	0.012, 0.010
	L&M	0.087, 0.014	0.120, 0.019	0.072, 0.020
	S	0.079, 0.013	0.068, 0.016	0.119, 0.009

Stimulus pattern		Binary noise	Sinusoidal
(Fig. 13)	A	0.041, 0.005	0.046, 0.006
	L&M	0.110, 0.022	0.135, 0.022
	S	0.107, 0.006	0.142, 0.022

about 0.10 along L & M cone and S cone axes correspond to contrast fluctuations of about 0.0088 to L cones and 0.089 to S cones, respectively, about the chosen mean contrasts of 0.044 to L cones and 0.445 to S cones, respectively. The induced contrast modulations at isoluminance are easily seen and appear as modulations of color saturation.

Each data point represents the average null from four observers: the error bars represent the estimated SEM. The intervals of uncertainty for each null plotted in Fig. 4, averaged across the observers, are presented in Table 1. Each observer judged the quality of the nulls excellent: the disk did not fluctuate in appearance at the null.

The three curves show that the amount of modulation needed to null the induced effect increases as the inducing contrast modulation increases. Along achromatic, L & M cone and S cone axes, there is little increase in the induced modulation beyond an annulus contrast modulation of 0.3. That the saturation in the effect occurs at the same level on the three color space axes is accidental, given the choice to scale contrasts according to the maximum available along each axis.

Disk mean contrast

If the effect of annulus contrast modulation on disk appearance is to modulate disk contrast, then reducing the disk contrast to zero should eliminate all effects of
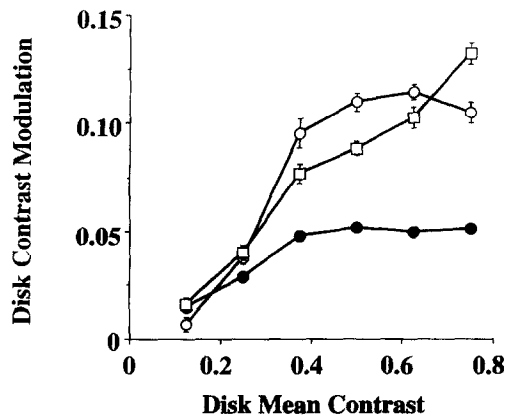
FIGURE 5. Results of varying the mean contrast of the disk, shown for achromatic stimuli (●), L & M cone axis stimuli (○) and S cone axis stimuli (□). Annulus mean contrast was fixed at 0.5. See caption to Fig. 4 and text for further discussion; nulls and intervals of uncertainty are listed in Table 1.
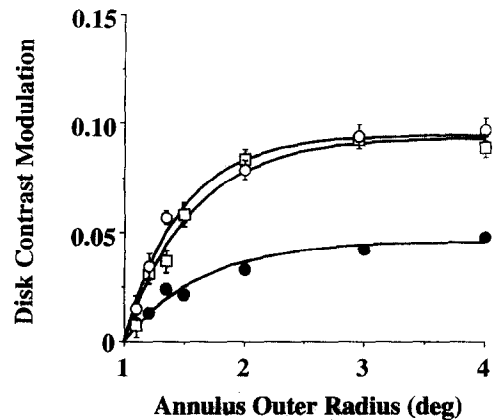

FIGURE 6. Results of varying the outer radius of the annulus, shown for achromatic stimuli (●), L & M cone axis stimuli (○) and S cone axis stimuli (□). The area of the annulus with inner radius 1 deg increases as the outer radius is increased (left to right). Smooth curves are best-fitting solutions to equation (1); parameters for the fits are listed in Table 2. Disk and annulus mean contrast was fixed at 0.5. See caption to Fig. 4 and text for further discussion; nulls and intervals of uncertainty are listed in Table 1.

annulus contrast modulation. Informal observations of the effects of annulus contrast modulation on uniform gray disks confirmed this expectation; contrast modulation along achromatic, L & M cone and S cone axes did not alter the appearance of a uniform disk with the chromatic properties of the gray background. We investigated the role of disk contrast more systematically by measuring the magnitude of induced modulation as a function of disk mean contrast.

The results show that nulling contrast modulations decrease towards zero as disk mean contrast decreases towards zero along achromatic (solid circles), L & M cone (open circles) and S cone (open square) axes (see Fig. 5). The annulus mean contrast was 0.5, as before, and annulus contrast modulations were fixed at 0.5. Induction saturates at disk mean contrasts of 0.375 and above to achromatic and L & M cone axis stimuli. For S cone stimuli, induction increases up to disk mean contrasts of 0.75.

These two experiments show that there are contrast gain control mechanisms, operative at isoluminance, which act rapidly to adjust the appearance of color contrast in response to physical changes in contrast. Mechanisms of chromatic adaptation that adjust sensitivity in response to changes in mean light levels provide an unlikely account of the results, because average lights from small areas of the stimulus are set to the background gray throughout the present experiments (see Fig. 1). Likewise, the rapid, reversible adjustment of appearance demonstrated here speaks against mediation of the effect by habituation (Krauskopf *et al.*, 1982, 1986b).

Annulus size

Quantitative accounts of contrast gain control invoke mechanisms that use local measures of contrast energy to set gain (Sperling, 1989; Heeger, 1991). The models lead one to expect that color contrast modulation in areas adjacent to the central disk induces more contrast modulation than does contrast modulation in distant areas.

We measured how the strength of color contrast induction depends on the distance of the inducing area from the central disk in two experiments. In the first, we varied the outer radius of the annulus from a value just larger than the 1 deg radius of the central disk up to the 4 deg radius of the standard annulus. For each color space axis, the mean contrast and the contrast modulation of the annuli were fixed at 0.5; the mean contrast of the central disk was also set to 0.5.

Figure 6 shows that, for stimuli along the achromatic (solid circles), L & M cone (open circles) and S cone (open squares) axes, the induction increases with increasing outer radius. The data points represent the average nulling contrast modulations for four observers. Following work on color induction (e.g. Tiplitz Blackwell & Buchsbaum, 1988), we have fit these data, for each color space axis, by an exponential $f(x)$ of the form

$$f(x) = S_{max} (1 - e^{-\alpha x}), \tag{1}$$

in which x is the annulus ring width, namely the outer radius minus 1 deg of visual angle, α is a space constant that sets the rate at which induction increases as outer radius increases, and S_{max} is the asymptotic nulling contrast modulation. Table 2 contains the estimated values of S_{max} and α for stimuli along each color space axis. These were determined using the computer routine praxis (Powell, 1964; Brent, 1973; Gegenfurtner, 1993). The estimates of the space constants for the three color space axes lie in a range of 0.5 deg and average 1.81 deg of visual angle.

TABLE 2. Parameters for the fit to data in Fig. 6 by equation (1)

	A	L&M	S
S_{max}	0.046	0.095	0.094
α	1.543	2.115	1.773

Distance of contrast modulation

The results of varying annulus size suggest how the efficacy of contrast modulation falls off with distance. Yet the preceding measurements confound area and position of contrast modulation. Although unlikely, it is possible that the areas in which contrast was modulated produced effects that were independent of the area's position relative to the central disk.

We linked position of contrast modulation to induction more firmly in a second experiment, in which we modulated contrast within rings of identical area about the central disk (see Fig. 7). The area between the modulated ring and the central disk was set to the uniform gray of the background. One expects that as the inner radius of such a ring increases, so that the contrast modulation is made more distant from the central disk, induction will decrease. Figure 7 shows the results of this experiment along the achromatic, L & M cone and S cone axes. For each axis, the mean contrast and the contrast modulation of the annuli were fixed at 0.5; the mean contrast of the central disk was also set to 0.5. Rings of area 3π deg^2 of visual angle were used. The figure shows the average results from the three observers LD, JL and BS.

The strength of color contrast induction falls off roughly exponentially with increasing distance of the ring from the central disk. For each color space axis, the data points are fit well by an exponential $g(x)$ of the form
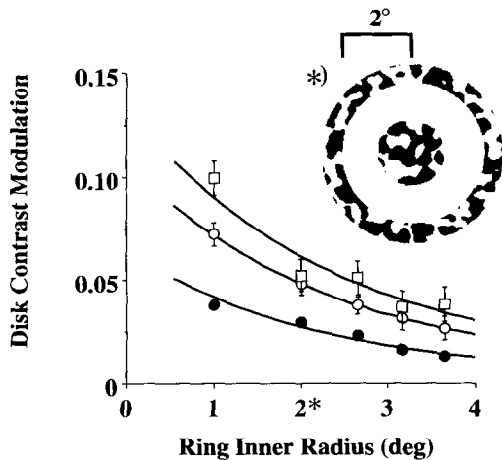
$$g(x) = T_{max}\ e^{-\beta x},\qquad(2)$$

FIGURE 7. Results of varying the distance of modulating contrast from the central disk, shown for achromatic stimuli (●), L & M cone axis stimuli (○) and S cone axis stimuli (□). The inner and outer radii of the annulus were varied to produce rings of constant area 3π deg^2. The distance of the rings from the central test disk increases as the inner radius is increased (left to right). The inset shows the spatial configuration of the stimulus with 2 deg inner radius; the area between the ring and the central disk was set to the neutral gray of the background. Average nulls and estimated SEMs are shown for the three observers LD, JL and BS. Smooth curves are best-fitting solutions to equation (2); parameters for the fits are listed in Table 3. Disk and annulus mean contrast was fixed at 0.5. See caption to Fig. 4 and text for further discussion; nulls and intervals of uncertainty are listed in Table 1.

TABLE 3. Parameters for the fit to data in Fig. 7 by equation (2)

	A	L&M	S
T_{max}	0.062	0.104	0.128
β	0.405	0.375	0.364

in which x is the ring inner radius, β is a space constant that sets the rate at which induction decreases as ring inner radius increases, and T_{max} is the maximum nulling contrast modulation. Table 3 contains the estimated values of T_{max} and β for stimuli along each color space axis.

The nulls found with rings of inner radius 1 (Fig. 7) should match nulls for annuli of outer radius 2 (Fig. 6), because the stimuli are identical. This is true, within the limits of measurement accuracy. Contrast induction decreases as ring inner radius increases. Yet rings with larger inner radii induce more contrast modulation than one might expect, given the results with the annuli. The differential affect of added annulus area is very small beyond 2 deg of visual angle (Fig. 6), yet disk contrast modulation caused by rings at 2 or more deg is substantial (Fig. 7). This persistence of induced contrast modulation as ring inner radius increases suggests that a contrast modulation edge at some distance may induce contrast modulation more strongly than an additional area of contrast modulation at the same distance. A similar suggestion for brightness and color contrast was made by Yund and Armington (1975).

Relative spatial orientation of annulus and disk noise patterns

The effect of contrast modulation may vary not only with spatial position but also with spatial frequency and orientation. The present stimuli, binarized differences of Gaussians, are not sufficiently localized in the spatial frequency domain to warrant an examination of the spatial frequency specificity of color contrast gain control, like that done by Chubb et al. (1989) with achromatic stimuli. Yet we did adapt the stimuli to a study of orientation specificity. We multiplied the two-dimensional amplitude spectra used to generate the stimuli (see Methods) by "sector" functions that eliminated energy at all orientations outside some particular sector of the spatial frequency domain. The remaining energy was limited in orientation in a way that was controlled by the width and position of the sector.

We used disks and annuli with orientation sectors of width 30 deg, admitting contrast energy within a band ± 15 deg of some mean orientation. The mean orientation of the disks was held at 0 deg (horizontal noisy bars) throughout the experiment; the mean orientation of the annuli varied from 0 through 150 deg in 30 deg increments (see Fig. 8). For each color space axis, the mean contrast and the contrast modulation of the annuli were fixed at 0.5; the mean contrast of the central disk was also set to 0.5.

As shown in Fig. 8, induced contrast modulation was fairly constant, for each color space axis, as annulus
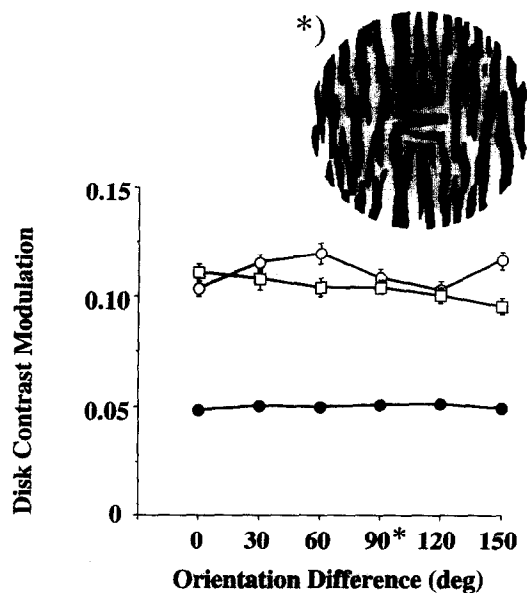
FIGURE 8. Results of varying the relative spatial orientation of disk and annulus noise patterns, shown for achromatic stimuli (●), L & M cone axis stimuli (○) and S cone axis stimuli (□). Annulus mean orientation varied from 0 through 150 deg (horizontal axis); disk mean orientation was fixed at 0 deg (horizontal). The inset shows the spatial configuration of the stimulus with a disk orientation of 0 deg and an annulus orientation of 90 deg. Disk and annulus mean contrast was fixed at 0.5. See caption to Fig. 4 and text for further discussion; nulls and intervals of uncertainty are listed in Table 1.
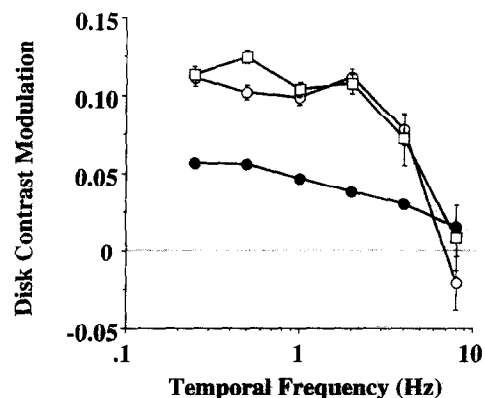

FIGURE 9. Results of varying the temporal frequency of the annulus contrast modulation, shown for achromatic stimuli (●), L & M cone axis stimuli (○) and S cone axis stimuli (□). Nulling contrast modulations were determined for contrast modulation rates of 0.25, 0.5, 1.0, 2.0, 4.0 and 8.0 Hz. Disk and annulus mean contrast was fixed at 0.5. See caption to Fig. 4 and text for further discussion; nulls and intervals of uncertainty are listed in Table 1.

pattern orientation was varied relative to the orientation of the central disk pattern. This lack of orientation specificity suggests that if contrast energies used for gain control are pooled across mechanisms that are tuned to a variety of orientations (e.g. Heeger, 1991), then these energies are pooled with equal weight per unit of orientation. In other words, the results suggest that the contrast measures used to set gain for achromatic, L & M cone and S cone axis contrasts are spatially isotropic. As mentioned in the Discussion, the results of Solomon, Sperling and Chubb (1993) suggest that this conclusion is likely to hold true with chromatic stimuli only at lower spatial frequencies.

Temporal frequency of contrast modulation

Contrast induction can be demonstrated using static patterns that are either achromatic (Chubb et al., 1989) or isoluminant. The latter can be demonstrated by placing side-by-side on a gray background two of the isoluminant binary noise stimuli with, say, L & M cone axis chromaticities. Set one annulus to a high contrast and the other to a low contrast; set the central disks to an intermediate contrast. Contrast induction at isoluminance is demonstrated by the marked difference in the apparent contrasts of the central disks: the disk surrounded by high contrast appears to have a lower color contrast than the disk surrounded by low contrast.

The demonstration of contrast induction using static patterns suggests that the responsible mechanisms have a substantial sensitivity to contrast energy at low temporal frequencies. This is supported by the results of experiments in which we varied the temporal frequency

of the contrast modulation (see Fig. 9). We varied the rate of contrast modulation from 0.25 through 8 Hz. Annulus and disk mean contrasts were 0.5; the annulus modulation was 0.5.

The temporal tuning curves have lowpass shapes for achromatic (solid circle), L & M cone (open circle) and S cone (open square) axis stimuli. The amounts of contrast modulation that are required to null the induced modulation decrease, with some fluctuation, as the temporal frequency of the inducing modulation increases. The sensitivity to isoluminant contrast modulation falls off above 2 Hz; sensitivity to both achromatic and isoluminant contrast modulation cuts off at about 8 Hz. The results provide no evidence for bandpass temporal frequency tuning of contrast gain control mechanisms. The lowpass sensitivities are like those found by DeValois et al. (1986) for first-order brightness and color induction.

Intervals of uncertainty were large at 4 Hz and especially at 8 Hz with the isoluminant stimuli (see Table 1). The estimated SEMs for the four observers at 4 and 8 Hz shown in Fig. 9 reflect the increasing difficulty in judging nulls at these temporal frequencies. Observers reported that it was often difficult to identify the phase of disk modulations at these higher temporal frequencies.

Temporal phase of nulling contrast modulation

We attempted to measure the phases of the best nulling modulations along the three cardinal axes at 1, 2 and 4 Hz. We wanted to ascertain that the phase of 0 deg, used to null the 1 Hz stimuli in most of these experiments, was the best choice. We also wanted to estimate the speed with which color constant induction propagates across the visual field.

The three observers LD, KH and BS participated in the experiments. The observers first determined the amplitudes of the nulling modulations presented with a phase of zero. These amplitudes were then held steady

while the phase of candidate nulling modulations was varied in experiments using the method of limits. Observers responded according to whether the central disk appeared steady or not. Descending sequences commenced with phase advances sufficiently large to be reported as not steady. Phases were decreased through zero to become phase lags. At some point, observers' responses shifted from not steady to steady. Responses again shifted, from steady to not steady, with increasing lag.

The attempt to measure phase suffered problems with precision and with plausibility (see Fig. 10). First, the intervals of uncertainty, which are recorded in Table 1, are large and show that there is a substantial range of phases, of breadth approx. 60 deg, that can be perceived as steady under the conditions of measurement. Second, the average phases represented by four of the data points are (noncausal) phase advances. This is so for measurements along the achromatic axis at 1, 2 and 4 Hz and along the S cone axis at 1 Hz.

Yet the results of two-tailed t-tests suggest that phases at 1 Hz differ significantly from zero along *no* axis. Along the achromatic axis, $t(2) = 2.15$ and $P > 0.10$ at 1 Hz, along the L & M cone axis, $t(2) = 0.43$ and $P > 0.20$ at 1 Hz, and along the S cone axis, $t(2) = 1.99$ and $P > 0.10$ at 1 Hz. The lack of significance suggests that our choice to use candidate nulling modulations of phase zero in the standard measurement procedure is an appropriate choice.

Furthermore, none of the implausible phases, in the four conditions where the average phase represents a phase advance, were significantly different from zero. In addition to the results mentioned above for the achromatic and S cone axes at 1 Hz, we find that along the achromatic axis, $t(2) = 0.44$, $P > 0.20$ at 2 Hz, and $t(2) = 0.21$, $P > 0.20$ at 4 Hz.

Statistical tests show that there is a significant linear dependence of phase on temporal frequency for the isoluminant stimuli. This is not true for the results with achromatic stimuli. We used the results of three observers per condition in an ANOVA along each color space axis. We found a significant linear dependence of phase on temporal frequency for L & M cone axis stimuli [$F(2,4) = 8.57$, $P < 0.05$], for S cone axis stimuli [$F(2,4) = 16.47$, $P < 0.025$], but not for achromatic stimuli [$F(2,4) = 2.80$, $P > 0.10$]. We take up the lack of significance for achromatic stimuli in the Discussion. Note well that in performing these t-tests we have assumed that the midpoints of the (large) intervals of uncertainty are the best point estimates of the null phases. This need not be true, of course, and the results of these t-tests are, at best, suggestive.

One can use the best-fit lines to the data in the isoluminant conditions to estimate the speed with which color contrast induction propagates across the visual field. The parameters for the lines of Fig. 10 are listed in Table 4. The ability to fit such data with a line is consistent with a model in which phase lag is due to propagation of contrast induction at some fixed speed across the visual field. If we assume that there is a single distance across which contrast induction propagates in the present experiments—for purposes of approximating propagation speed—then we can use the slope of the best-fit line to estimate propagation speed in deg of visual angle per sec according to the shift theorem (Bracewell, 1978). The results of varying annulus size and ring diameter lead us to choose the relevant distance to be that between the disk-annulus edge and the disk center, namely 1 deg of visual angle. The slope of approx. -5 deg per Hertz found with the isoluminant stimuli (Table 4) then suggests a propagation speed of about 72 deg of visual angle per second. The short propagation distance used in the calculation suggests that this speed estimate may be a bit low.

Interocular transfer

We wanted to learn whether color contrast induction transfer interocularly, as a positive result would implicate cortical visual mechanisms in contrast gain control (Blakemore & Campbell, 1969). Although Chubb *et al.* (1989) found no interocular transfer using intermittently flashed dynamic noise stimuli, we suspected that one could demonstrate transfer using simpler methods.

A satisfactory demonstration of interocular transfer is provided by presenting the annulus on the left half and the disk on the right half of the color display and viewing these steadily through a stereoscope, so presenting in proper alignment the annulus to the left eye and the disk to the right eye. Modulating annulus contrast induces
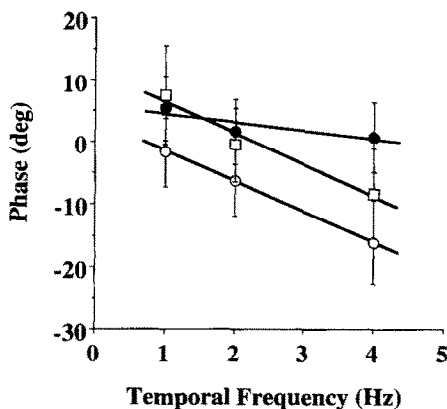

FIGURE 10. Results of phase lag determination, shown for achromatic stimuli (●), L & M cone axis stimuli (○) and S cone axis stimuli (□). Observers BS, LD and KH initially determined the amplitudes of the nulling contrast modulations along each axis at 1, 2 and 4 Hz. Disk and annulus mean contrasts were fixed at 0.5. Observers then found the nulling phases at these amplitudes using the method of limits. Plotted are the average nulls for the three observers; the error bars represent estimates of the SEMs. The slopes and intercepts of the best-fit lines to each color space axis' data are listed in Table 4. Average phases and intervals of uncertainty are listed in Table 1.

TABLE 4. Estimates of slopes m and intercepts b for temporal phase data

	A	L&M	S
m	-1.41	-4.81	-5.10
b	5.82	3.15	11.40

a modulation of disk apparent contrast. Interocular transfer occurs with achromatic, L & M cone axis and S cone stimuli.

We formalized the observations with an experiment. In one set of conditions (interocular), observers used the stereoscope (Stephens Scientific Products) to view the annulus through the left eye and the disk through the right, as in the demonstrations, and determined their nulls in the standard way. In a second set of conditions (monocular), both annulus and disk were presented on the left side of the display and were viewed through the stereoscope. The left eye alone was presented the disk and annulus; the right eye viewed the gray background.

Each trial was preceded by a presentation of the disk and annulus with physically steady contrast. In the interocular condition, observers used the steady display to ascertain non-rivalrous visibility of disk and annulus. When satisfied with the display, observers initiated the trial by pressing a key.

Results are shown in Fig. 11. The results compare interocular contrast induction (white bars) and monocular contrast induction (shaded bars) along achromatic (left), L & M cone (middle) and S cone axes (right). The heights of the bars represent the average nulls for the three observers MD, KH & BS, and they show that interocular and monocular nulls are comparable in magnitude. We used the results to perform one-tailed t-tests of the significance of the nulling contrast modulations determined for interocular presentation along each axis. Along the achromatic axis, $t(2) = 13.33$ and $P < 0.005$, along the L & M cone axis, $t(2) = 5.38$ and $P < 0.025$, and along the S cone axis, $t(2) = 9.17$ and $P < 0.01$; the results for interocular transfer are statistically significant.
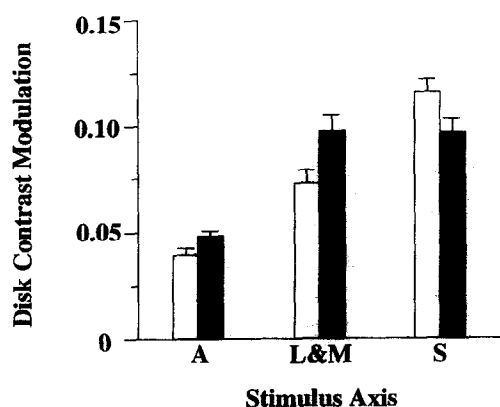

FIGURE 11. Results of experiment on interocular transfer of color contrast induction shown for each cardinal axis (achromatic, leftmost two bars; L & M cone, central two bars; S cone, rightmost two bars). Observers MD, KH and BS viewed the annulus in the left eye and the disk in the right eye in a first condition (white bars), and viewed both the annulus and the disk in the left eye in a second condition (shaded bars). Disk and annulus mean contrasts were fixed at 0.5; the annulus contrast modulations were 0.5. The heights of the bars represent the average nulls for the three observers; the error bars represent estimates of the SEMs. Average nulls and intervals of uncertainty are listed in Table 1.

The results of the experiment support the informal observations by showing a robust interocular transfer of contrast induction for achromatic, L & M cone and S cone axis stimuli. This positive result suggests that there are mechanisms in the human visual system which control contrast gain that have a cortical locus.

Color selectivity

We investigated chromatic selectivity in experiments that pit the three cardinal axes of Krauskopf against each other. We wanted to see, for instance, whether contrast modulation along the achromatic axis affects the appearance of contrast along the L & M cone axis.

Note that the nulling technique used in the previous experiments need not work in cases where annulus and disk have different chromatic properties. Consider an achromatic annulus and an isoluminant L & M cone axis disk. Suppose that modulating the contrast of the achromatic annulus has an effect on the red/blue-green appearance of the L & M cone axis disk. What might this effect be? Induction might cause the disk to be modulated in appearance along a red/blue-green direction, so that the nulling modulation lies along the L & M cone axis. Yet it is possible that the appearance of the red/blue-green disk fluctuates along the achromatic axis. Indeed, the appearance of red/blue-green disk may fluctuate along some intermediate axis or along some non-axial path in color space.

With the cardinal axis stimuli, we have found that we can null induced effects by modulating disk contrast along the color space axis of the disk. To conclude the example above, modulating the contrast of the achromatic annulus causes an L & M cone axis disk to be modulated in appearance along a red/blue-green direction and the nulling modulation lies along the L & M cone axis. We chose disks and annuli to have mean contrasts of 0.5 and the annulus contrasts to be modulated fully (0.5). Figure 12 shows the results with stimuli along the three cardinal axes.

The three bars at the left show the contrast modulations needed to null the modulation induced by achromatic annuli in achromatic disks, L & M cone axis disks and S cone axis disks. The achromatic contrast modulation has a significant effect on apparent contrast along all axes. The three bars in the center show the results of modulating the contrast of an L & M cone axis annulus. The modulation has no significant effect on the apparent contrast of an achromatic disk. It has a substantial effect on disks along the same color space axis and a lesser effect on S cone axis disks. The three bars at the right show the results of using an S cone annulus contrast modulation. The effect on achromatic disks is small. There is a substantial effect on disks along the same color space axis and a lesser effect on L & M cone axis disks.

The results show that modulating isoluminant contrast has little effect on achromatic contrast. Furthermore, the interaction found with completely isoluminant stimuli suggests that there is a partial
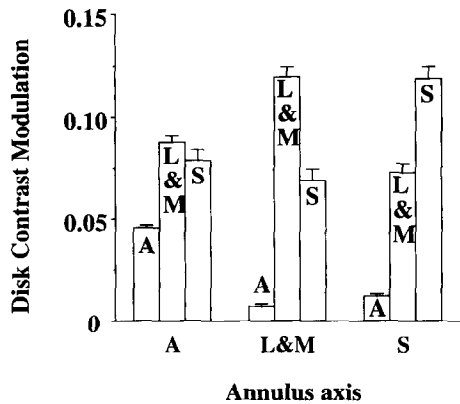
FIGURE 12. Results of varying disk and annulus chromatic properties independently, using cardinal axis stimuli. Annuli of mean contrast 0.5 with contrast modulation amplitudes of 0.5 were presented along each cardinal axis (achromatic axis, leftmost three bars; L & M cone axis, central three bars; S cone axis, rightmost three bars). For each choice of color space axis for the annulus, observers determined nulling contrast modulations for disks along each color space axis. The bar labels identify the color space axis of the disk. Bar heights represent the average nulling contrast modulations determined for five observers; error bars represent the average nulling contrast modulations determined for five observers; error bars represent estimates of the SEMs. Disk mean contrasts were fixed at 0.5. Nulls and intervals of uncertainty are listed in Table 1.

chromatic selectivity among color contrast gain control mechanisms. This interaction shows that contrast modulation along one axis affects apparent contrast more strongly along the same axis than along a different axis. This partial chromatic selectivity is like that found by Webster and Mollon (1991) in experiments on chromatic habituation.

Contrast modulation with spatially-sinusoidal patterns

The edges in the isoluminant binary noise patterns in these experiments produce luminance artifacts. Vertical edges are not reproduced precisely by raster monitors, so that nominally isoluminant stimuli may present luminance shadows at such edges. Because we do not use an achromatizing lens (Powell, 1981) in combination with cycloplegia, the edges also introduce artifacts associated with chromatic aberration (von Helmholtz, 1924; LeGrand, 1967; Van Meeteren, 1974; Thibos, Bradley, Still, Zhang & Howarth, 1990). The change in focus with wavelength causes longitudinal chromatic aberration (Wald & Griffin, 1947; Hopkins, 1962; Campbell & Gubisch, 1967; Charman & Jennings, 1976; Gilmartin & Hogan, 1985), which starts to corrupt spatially-sinusoidal isoluminant stimuli at frequencies beyond 4–6 c/deg (Mullen, 1985). The edges in our binary noise stimulus patterns cause them to present energy at higher spatial frequencies. The change in magnification with wavelength causes lateral chromatic aberration (Howarth, 1984; Simonet & Campbell, 1990; Zhang, Bradley & Thibos, 1993), which corrupts especially vertically-oriented isoluminant stimuli in foveal viewing.

We attempted to control for these artifacts by measuring induction with horizontally-oriented sinusoids of

frequency 2 c/deg (see Fig. 13, top). This frequency is close to the average peak frequency estimate of the binary noise stimuli, 1.8 c/deg. Raster artifacts and chromatic aberration are negligible for such sinusoids. The mean contrasts of disk and annulus and the phases of annulus and disk sinusoids were chosen to be identical to minimize the otherwise unavoidable annulus-disk edge artifact.

If contrast induction were found to be negligible at isoluminance using the sinusoidal stimuli then we would be forced to conclude that our results with the binary noise stimuli were due largely to luminance artifacts. On the other hand, if results using the sinusoidal stimuli were similar to those found using the binary noise stimuli, then we would be more confident that artifacts did not compromise our ability to characterize color contrast induction.

Three observers (MD, JL and BS) participated in the control experiment. Figure 13 shows the results of
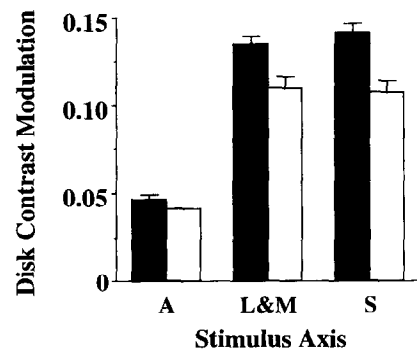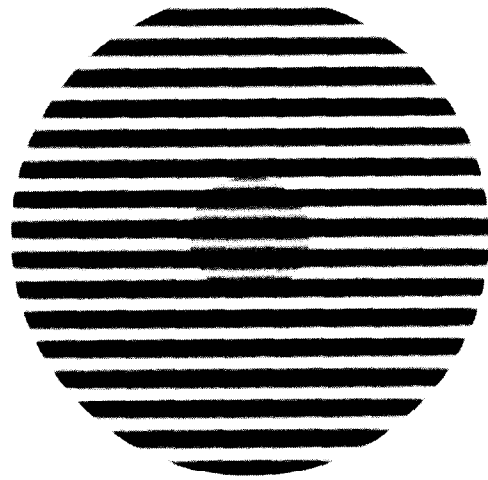

FIGURE 13. Results for spatially-sinusoidal stimuli (black bars) compared to results for binary noise stimuli (white bars), for the three observers MD, JL and BS. Annuli comprising spatial sinusoids at 2 c/deg of mean contrast 0.5 with contrast modulation amplitudes of 0.5 were presented along each color space axis (achromatic axis, left; L & M cone axis, center; S cone axis, right). For each annulus axis, observers determined nulling contrast modulations for sinusoidal-pattern disks along the same axis. The top part shows the spatial configuration of the spatially-sinusoidal stimuli. The bar heights represent the average nulling contrast modulations determined for the three observers; error bars represent estimates of the SEMs.

contrast induction measurements using sinusoids. For each color space axis the mean contrast and the contrast modulation of the annuli were fixed at 0.5; The mean contrast of the central disk was also set to 0.5. Figure 13 shows, for stimuli along the achromatic (left), L & M cone (center) and S cone axes (right), that the magnitudes of contrast induction found using sinusoids (black bars) are similar to the magnitudes found using binary noise (white bars). Indeed, the induction found using sinusoids is somewhat greater than that found using the comparable binary noise patterns. The data suggest that the results found with binary noise stimuli along the L & M cone and the S cone axes characterize chromatic mechanisms of contrast induction.

Contrast modulation with dynamic noise

Finally, we ruled out the possibility that the contrast induction effects are artifacts of modulating the contrast of static, spatial noise. Perhaps the effects that we attribute to contrast induction depend, in our experiments, on special patterns of eye movements, or on figural cues, such as constant adjacency relationships between pattern elements across the disk-annulus boundary. Such problems of interpretation are eliminated by using dynamic noise stimuli, like those of Chubb et al. (1989). Can induced contrast modulation be demonstrated at isoluminance using dynamic noise stimuli?

Dynamic noise stimuli were generated using software on a DECstation 3000/400, which controlled the sequential display of 256 × 256 pixel portions of off-screen memory by a Turbo PXG graphics board, which was set to provide 24 bits of chromatic information per pixel. Each frame held a binary noise pattern stimulus like that used in the previous experiments but half the physical size. Each frame possessed its own random phase spectrum, so that the binary noise pattern differed from frame to frame. Sixteen such frames were created and presented sequentially in the center of the Sony GDM-1961 color display at 64 msec intervals. Annulus contrast was modulated to provide a single sinusoidal cycle over the course of the 16 frames; the result was a dynamic noise stimulus with annulus contrast modulated sinusoidally at about 1 Hz.

We used these stimuli to make coarse measurements of the magnitude of color contrast induction. As in our first experiment on annulus contrast modulation, disk and annulus mean contrasts were fixed at 0.5. Two observers (the authors) used the method of adjustment to determine the nulling modulation needed along the achromatic, L & M cone and S cone axes when the annulus contrast was modulated maximally (0.5) along the same axis.

The induction of contrast modulation with achromatic and isoluminant dynamic noise stimuli is strong. For observer BS, the nulling modulations are about 0.08, 0.09 and 0.11 for achromatic, L & M cone and S cone axis stimuli, respectively, while those for MD are about 0.10, 0.14 and 0.14. These modulations are some-

what larger in magnitude than those found using static noise stimuli. The results of this control experiment suggest that the results with static noise stimuli are generally pertinent to stimuli in which contrast is modulated.

IV. DISCUSSION

These experiments have documented the presence of contrast gain control mechanisms that are sensitive to isoluminant modulations of contrast and have surveyed their basic properties.

Intensive properties

The results of the experiments on the intensive properties of color contrast induction show that the magnitude of induction increases approximately linearly with increasing contrast modulation and with increasing disk mean contrast, up to a point of saturation.

With static achromatic stimuli, the peak induced contrast modulation is nulled by a modulation of size approx. 0.05, while in our (final) experiment with dynamic noise stimuli, the achromatic nulling modulation was closer to 0.10. These values are smaller than the value of about 0.20 found by Chubb et al. (1989) with dynamic noise stimuli. Two factors may account for the difference in magnitude. First, our experiment on temporal frequency sensitivity shows that the underlying mechanisms have a lowpass sensitivity. One expects that the lower temporal frequency of contrast modulation chosen by Chubb et al. (0.47 vs 1 Hz) would give rise to a slightly larger effect. The second is the difference in stimulus spatial parameters. First, Chubb et al. used a disk 1.35 deg in diameter centered in a 3.6 deg square field, while we used larger stimuli, namely, a 2 deg disk in an annulus of diameter 8 deg. In addition, the peak spatial frequencies of their noise stimuli were two or more times greater than that in the present experiments (2.0 c/deg). These differences in stimulus spatial parameters may underlie the differences in null magnitudes, though just how we do not know.

The magnitudes of the nulls found for achromatic contrast induction by us and by Chubb et al. are substantially smaller than the nulls found in the experiments on simultaneous color induction by Krauskopf, Zaidi and Mandler (1986a). In those experiments, the annulus and disk were not patterned but spatially uniform. For one observer in those experiments, the peak nulling amplitude was about 0.5 for achromatic stimuli, while for the other observer it was about 0.9. A somewhat smaller value of 0.3 was reported by DeValois et al. (1986) in their matching experiments on brightness and color induction, but this was found with an inducing modulation of 0.6. Of course, it is not surprising that the present results on the response of the visual system to changes in contrast about some average light level differ from the results of experiments on the response of the visual system to changes in average light levels.

Spatial properties

We explored the spatial properties of color contrast induction in three experiments. We were guided by results from experiments on spatial parameters in brightness and color induction (Kirschmann, 1890; Jameson & Hurvich, 1961; Kinney, 1962; Oyama & Hsia, 1966; Wässle & Heinrich, 1970; Walraven, 1973; Yund & Armington, 1975; Tiplitz Blackwell & Buchsbaum, 1988; Zaidi, Yoshimi, Flanigan & Canova, 1992) and by models of contrast gain control (Sperling, 1989, Heeger, 1991).

Our results with spatial parameters show that (1) contrast induction increases as inducing area increases and that (2) contrast induction decreases as the distance of the inducing area increases. We found that expressions involving exponentials can be used to describe the data adequately, and that the space constants for the exponential fits are roughly independent of stimulus color space axis. For the experiment in which annulus area was varied, the space constants ranged from 1.5 to 2.1 deg of visual angle and averaged about 1.8 deg (Table 2), while for the experiment in which annulus inner radius was varied, the space constants ranged from 0.36 to 0.41 deg of visual angle, with an average of about 0.38 deg (Table 3).

The difference in space constants across the two experiments reflects the difference in design and in the fitted expressions. The similarity of space constants across color space axes within individual experiments suggests that chromatically-arbitrary contrast modulations are unlikely to lead to a space-varying change in the apparent chromatic contrast properties of neighboring regions. For instance, a small space constant for achromatic contrast and a large one for isoluminant contrast could lead a contrast modulation with components along both achromatic and isoluminant axes to cause a significant reduction in apparent color contrast, but not achromatic contrast, at a far enough distance. The results suggest that this source of differential induction is minimal.

Our results for the spatial parameters of color contrast induction are like those of earlier work on brightness and color induction.

Several investigators explored the increase in brightness and color induction as a function of inducing field area. An early study was performed by Kirschmann (1890), who concluded tentatively that color contrast induction increases as inducing area increases. Kinney (1962) found that as the size of a colored inducing field increases relative to that of a test field with the chromaticity of Illuminant A (Wyszecki & Stiles, 1982), so does the induced color shift. Wässle and Heinrich (1970) used a test square of width 1 deg to show that brightness induction increases as the size of an inducing square region increases. They found that induction saturates at about the point where the inducing block's width reaches 2 deg. Walraven (1973) found that increasing the size of an inducing annulus increases the amount of red light that has to be added to a flashing yellowish test ring in

order for the ring to remain yellow. The induction saturates at inducing field diameters between 2 and 3 deg. Yund and Armington (1975) found that increasing annulus size leads to increases in the intensity of a monochromatic light that must be added to a matching stimulus for it to match a central test stimulus in hue. Tiplitz Blackwell and Buchsbaum (1988) used isoluminant stimuli and found an exponential relation between surround size and the change in 1960-CIE UCS coordinates u and v between the test square and a match square presented simultaneously elsewhere in the visual field.

The effect of distance between test region and inducing area also affects induced brightness and color, an effect noted by Kirschmann (1890) and quantified by Jameson and Hurvich (1961) in terms of inducing and focal area contiguity. Oyama and Hsia (1966) found that as the distance between a 4 deg circular test and the inner radius of an inducing surround increases from 0 to 8 deg, the hue shift required to maintain a constant test hue decreases. In their exploration of brightness induction, Wässle and Heinrich (1970) found that increasing the separation between test and inducing areas leads to a decrease in induction that is nearly minimal for separations beyond 1.5 deg. Walraven (1973) found that the amount of red light that must be added to a flashing yellowish test ring in order for it to remain pure yellow falls off in an approximately exponential way with increasing annulus inner radius. Tiplitz Blackwell and Buchsbaum (1988) found that increasing the separation between a 0.62 deg test square and an isoluminant rectangular ring from 0 to 0.25 deg causes a change in chromaticity coordinates, between the test square and a match square, to decrease in a way described well by a negative exponential. Zaidi et al. (1992) used circular gratings to determine spatial sensitivities for both brightness and color induction. They found that brightness induction is additive and has a spatial sensitivity that falls off exponentially, and that color induction is spatially nonlinear.

These results for color induction agree with our experiments on color contrast induction in showing that (1) induction increases as the inducing area increases and (2) induction decreases with increasing distance of the inducing area. Note that the specific space constants for contrast induction that we report here may well depend on the spatial frequency content of the contrast pattern (e.g. the grain of the noise). Such a dependence is suggested by the work of Cannon and Fullenkamp (1991), who, in agreement with the present results, found that the spatial pooling function for sinusoidal stimuli at 2 c/deg levels off exponentially between annulus outer diameters of 4 and 6 deg. Furthermore, in varying the inducing area and the distance of the inducing area, we simultaneously altered the spatial frequency properties of the inducing stimulus. We are currently investigating such alterations systematically in experiments that vary the spatial frequency content of the contrast pattern and the spatial frequency content of the contrast modulation.

Our results with oriented stimuli suggest that color contrast induction is spatially isotropic. This result is found using stimuli with high contrasts and low peak spatial frequencies, namely about 1.8 c/deg. Solomon *et al.* (1993) found orientation selectivity in achromatic contrast gain control using spatially-sinusoidal stimuli at 10 and 20 c/deg. They also found orientation selectivity at a spatial frequency of 3.3 c/deg when the stimuli were presented at low contrasts (<0.10). However, they found no orientation selectivity at 3.3 c/deg at higher contrasts, and this result agrees fully with our own for color contrast gain control.

Temporal properties

The temporal frequency sensitivity of the mechanisms responsible for contrast induction has a lowpass characteristic. The sensitivity functions for isoluminant stimuli have shoulders at about 2 Hz, and the sensitivities to stimuli along all three axes cut off at about 8 Hz. The phases of the best nulling modulations lag increasingly behind the inducing modulation as temporal frequency increases. While the best nulling phase at 1 Hz does not differ significantly from 0 deg, we found statistically significant phase lags at higher frequencies for isoluminant stimuli. We used these lags to estimate the propagation speed of color contrast induction to be about 72 deg/sec.

We have no reason to believe that the lack of significant change in phase with temporal frequency for achromatic stimuli is anything other than a problem of unreliable measurement. Were there a small phase lag (so implying a higher propagation speed) for achromatic stimuli, we would potentially be able to see achromatic contrast modulate before chromatic contrast in response to a sufficiently distant modulation of contrast with components along achromatic and isoluminant axes. Identical phase lags and speeds of propagation would minimize this source of differential induction.

The temporal frequency sensitivities that we found for color contrast induction are similar to those found for color induction by DeValois *et al.* (1986). They found lowpass shapes for the induced effects of both brightness and color modulation with sharp shoulders at 2.5 Hz. DeValois *et al.* argued that the very slow temporal characteristics of induction suggest a cortical site rather than a retinal one. Likewise, the similarity of the temporal properties of color and brightness induction suggests a single, later, cortical process which operates similarly on both brightness and color information. These arguments in favor of cortical sites apply also to color contrast induction.

There is no conclusive evidence from electrophysiological experiments on primates that the locus of color contrast induction is cortical. In cat, a fast contrast gain control was demonstrated in the retina by Shapley and Victor (1979), while Ohzawa, Sclar and Freeman (1985) showed that there are sites in cat cortex that habituate slowly to contrast, of the sort that one might expect from the psychophysical experiments of Blakemore and Campbell (1969). Geisler and Albrecht (1992)

found evidence for a fast-acting contrast gain contol that acts on simple cell responses in cat. In macaque, the slow form of contrast gain control (habituation) is evident in the responses of simple and complex cells in striate cortex (Sclar, Lennie & DePriest, 1989) but not in responses of neurons in lateral geniculate nucleus (Derrington & Lennie, 1984).

The lateral interactions in macaque V4 neuron receptive fields between large silent suppressive surrounds and small excitatory centers (Desimone, Schein, Moran & Ungerleider, 1985; Schein & Desimone, 1990) seem a plausible basis for brightness and color induction (Courtney, Finkel & Buchsbaum, 1994) and for color contrast induction, although a definite relationship remains to be shown.

Interocular transfer

We investigated the issue of locus directly in an experiment on the interocular transfer of color contrast induction. The experimental results show a robust transfer for stimuli along achromatic, L & M cone and S cone axes, and we conclude that there are cortical sites of rapid color contrast gain control in humans. We took care to ensure that both disk and annulus were simultaneously visible to observers for period of time long enough to make sound judgements of appearance. We do not know why Chubb *et al.* (1989) found a negative result. The major difference between the two experiments is that they flashed their stimuli for intervals of 133 msec every half a second, while we presented ours steadily. Perhaps cortical sites that mediate contrast induction are insensitive to briefly flashed stimuli; this agrees loosely with the sluggish temporal frequency sensitivities found in the previous experiment. That there are probably both retinal and cortical contributions to human brightness induction was shown by Shevell, Holliday and Whittle (1992); the same may be true for color contrast induction.

Chromatic selectivity

Our results on chromatic selectivity rule out two possible models of color contrast gain control. In a first model, which we call the "colorless energy" model, a single measure of contrast energy that combines both achromatic and chromatic contrast is used to control gain. In this model, the effect of any annulus is captured by a single number, its colorless energy, which is independent of test disk properties. When an annulus is modulated, this produces a change in colorless energy. The simplest form of this model holds that this change in colorless energy is related monotonically to change in contrast gain in achromatic and chromatic visual channels.

Comparing the results obtained with achromatic and L & M cone axis stimuli (see Fig. 12) speaks against the use of colorless energy in normalizing apparent contrast. According to the model, modulating the contrast of the achromatic axis annulus produces some change in colorless contrast energy. This change is either greater than that produced by modulating the L & M

cone axis annulus or it is not. The greater induction (0.045 vs 0.007) for achromatic disks found with achromatic modulation suggests that the change in colorless energy is greater, yet the decreased induction (0.087 vs 0.120) for L & M cone disks found with achromatic modulation suggests that it is less (see Fig. 12). This interaction, and that between achromatic and S cone axis stimuli, both of which were found in the results of all five observers, contradict the colorless energy model.

This conclusion is strengthened by the interaction obtained with L & M cone axis and S cone axis stimuli (see Fig. 12). According to the colorless energy model, modulating the contrast of the L & M cone axis annulus produces a change in colorless energy that is either greater than that produced by modulating the S cone axis annulus or not. The induction for L & M cone disks found with L & M cone modulation (0.120) is greater than that found with S cone modulation (0.072), which suggests that the change in colorless energy is greater for the L & M cone annulus modulation. Yet the induction for S cone disks found with L & M cone annulus modulation (0.068) is less than that found with S cone annulus modulation (0.119), which suggests that the change in colorless energy is greater for the S cone annulus modulation. The interaction between isoluminant stimuli, found in the results of each of the five observers, contradicts the colorless energy model.

The results also speak against a model in which each channel has its own independent contrast gain control. The induction along all axes that we have tested which is caused by the modulation of achromatic contrast, for instance, is not consistent with this model. Note that the results suggest a limited independence for achromatic stimuli: the regulation of apparent achromatic contrast seems to be controlled largely by achromatic contrast energy.

While our results provide no evidence in favor of chromatic channels that have independent contrast gain controls, the small number of color space axes that were tested leaves open the possibility that such channels exist. Preliminary data from our laboratory on chromatic selectivity in experiments that use stimuli along intermediate axes suggest that there are no channels that are completely independent. At present, we cannot rule out the possibility that higher-level, non-cardinal mechanisms tuned to intermediate color directions (Krauskopf et al., 1986a, b) play a role in color contrast induction. Furthermore, we cannot, at present, rule out the possibility that the relatively high levels of contrast and contrast modulation used in the present experiments cause a chromatic spread of gain control activation. It remains to be determined whether chromatic channels possess gain controls that act independently at low levels of contrast and contrast modulation.

REFERENCES

Arend, L. & Reeves, A. (1986). Simultaneous color constancy. *Journal of the Optical Society of America A*, *3*, 1743–1751.

Augenstein, E. J. & Pugh, E. N. (1977). The dynamics of the Π_1 colour mechanism: Further evidence for two sites of adaptation. *Journal of Physiology, London*, *272*, 247–281.

Bäuml, K.-H. (1994). Color appearance: The effect of illuminant changes under different surface collections. *Journal of the Optical Society of America A*, *11*, 531–542.

Blakemore, C. & Campbell, F. W. (1969). On the existence of neurones in the human visual system selectively sensitive to the orientation and size of retinal images. *Journal of Physiology, London*, *203*, 237–260.

Bracewell, R. N. (1978). *The Fourier transform and its application* (2nd edn). New York: McGraw-Hill.

Brainard, D. H. & Wandell, B. A. (1992) Asymmetric color matching: How color appearance depends on the illuminant. *Journal of the Optical Society of America A*, *9*, 1433–1448.

Brent, R. P. (1973). *Algorithms for minimization without derivatives*. Engelwood Cliffs, N.J.: Prentice-Hall.

Brown, R. O. (1993). Integration of enhanced-contrast edges in color vision. *Investigative Ophthalmology and Visual Science (Suppl.)*, *34*, 766.

Brown, R. O. & MacLeod, D. I. A. (1992). Saturation and color constancy. *Optical Society of America 1992 Technical Digest Series*, *4*, 110–111.

Campbell, F. W. & Gubisch, R. W. (1967). The effect of chromatic aberration on visual acuity. *Journal of Physiology*, *192*, 345–358.

Cannon, M. W. & Fullenkamp, S. C. (1991). Spatial interactions in apparent contrast: Inhibitory effects among grating patterns of different spatial frequencies, spatial positions and orientations. *Vision Research*, *31*, 1985–1998.

Charman, W. N. & Jennings, J. A. M. (1976). Objective measurements of the longitudinal chromatic aberration of the human eye. *Vision Research*, *16*, 999–1005.

Chubb, C., Sperling, G. & Solomon, J. A. (1989). Texture interactions determine perceived contrast. *Proceedings of the National Academy of Sciences U.S.A.*, *86*, 9631–9635.

Courtney, S. M., Finkel, L. H. & Buchsbaum, G. (1994). Network simulations of retinal and cortical contributions to color constancy. *Vision Research*. In press.

Derrington, A. M., Krauskopf, J. & Lennie, P. (1984). Chromatic mechanisms in lateral geniculate nucleus of macaque. *Journal of Physiology, London*, *357*, 241–265.

Derrington, A. M. & Lennie, P. (1984). Spatial and temporal contrast sensitivities of neurones in lateral geniculate nucleus of macaque. *Journal of Physiology, London*, *357*, 219–240.

Desimone, R., Schein, S. J., Moran, J. & Ungerleider, L. G. (1985). Contour, color and shape analysis beyond the striate cortex. *Vision Research*, *25*, 441–452.

DeValois, R. L., Webster, M. A., DeValois, K. K. & Lingelbach, B. (1986). Temporal properties of brightness and color induction. *Vision Research*, *26*, 887–897.

D'Zmura, M. & Lennie, P. (1986). Mechanisms of color constancy. *Journal of the Optical Society of America A*, *3*, 1662–1672.

Fairchild, M. D. & Lennie, P. (1992). Chromatic adaptation to natural and incandescent illuminants. *Vision Research*, *32*, 2077–2085.

Gegenfurtner, K. R. (1993). PRAXIS: Brent's algorithm for function minimization. *Behavior Research Methods, Instruments & Computers*, *24*, 560–564.

Geisler, W. S. & Albrecht, D. G. (1992). Cortical neurons: Isolation of contrast gain control. *Vision Research*, *32*, 1409–1410.

Gilmartin, B. & Hogan, R. E. (1985). The magnitude of longitudinal chromatic aberration of the human eye between 458 and 633 nm. *Vision Research*, *25*, 1747–1753.

Heeger, D. J. (1991). Nonlinear model of neural responses in cat visual cortex. In Landy, M. S. & Movshon, J. A. (Eds), *Computational models of visual processing* (pp. 119–133). Cambridge, Mass.: MIT.

von Helmholtz, H. (1924). *Treatise on physiological optics* (Vol. 1) (translated by Southall, M. P. C. from 3rd German edition). New York: Dover.

Hopkins, H. H. (1962). The application of frequency response techniques in optics. *Proceedings of the Physical Society*, *79*, 889–919.

Howarth, P. A. (1984). The lateral chromatic aberration of the eye. *Ophthalmology and Physiological Optics, 4* 223–226.

Ishihara, S. (1986). *The series of plates designed as a test for colour-blindness.* Tokyo: Kanehara.

Jameson, D. & Hurvich, L. M. (1961). Opponent chromatic induction: Experimental evaluation and theoretical account. *Journal of the Optical Society of America, 51*, 46–53.

Jenness, J. W. & Shevell S. K. (1993). Chromatic complexity and color appearance: A dark cloud over the gray world hypothesis. *Investigative Ophthalmology and Visual Sciences (Suppl.), 34*, 765.

Judd, D. B. (1940). Hue, saturation and lightness of surface colors with chromatic illumination. *Journal of the Optical Society of America, 30*, 2–32.

Kinney, J. A. (1962). Factors affecting induced color. *Vision Research, 2*, 503–525.

Kirschmann, A. (1890). Ueber die quantitativan Verhältnisse des simultanen Helligkeits- und Farben-Contrastes. *Philosophische Studien, 6*, 391–417.

Krauskopf, J., Williams, D. R. & Heeley, D. M. (1982). The cardinal directions of color space. *Vision Research, 22*, 1123–1131.

Krauskopf, J., Zaidi, Q. & Mandler, M. B. (1986a). Mechanisms of simultaneous color induction. *Journal of the Optical Society of America A, 3*, 1752–1757.

Krauskopf, J., Williams, D. R., Mandler, M. B. & Brown, A. M. (1986b). Higher-order color mechanisms. *Vision Research, 26*, 23–32.

von Kries, J. (1905). Influence of adaptation on the effects produced by luminous stimuli. *Handbuch der Physiologie des Menschen, 3*, 109–282. In Macadam, D. L. (Ed.), *Sources of color vision.* Cambridge, Mass.: MIT.

LeGrand, Y. (1967). *Form and space vision* (translated by Millodot, M. & Heath, G. G.). Bloomington, Ind.: Indiana University Press.

Loomis, J. M. (1980). Transient tritanopia: Failure of time-intensity reciprocity in adaptation to long-wavelength light. *Vision Research, 20*, 837–846.

MacLeod, D. I. A. & Boynton, R. M. (1979). Chromaticity diagram showing cone excitation by stimuli of equal luminance. *Journal of the Optical Society of America, 69*, 1183–1186.

McCann, J. J. (1989). The role of simple nonlinear operations in modeling human lightness and color sensations. *Proceedings of the SPIE—International Society of Optical Engineers 1077, Human Vision, Visual Processing, and Digital Display*, pp. 355–363.

Mullen, K. (1985). The contrast sensitivity of human colour vision to red–green and blue–yellow chromatic gratings. *Journal of Physiology, London, 359*, 381–400.

Ohzawa, I., Sclar, G. & Freeman, R. D. (1985). Contrast gain control in the cat's visual system. *Journal of Neurophysiology, 54*, 651–667.

Oyama, T. & Hsia, Y. (1966). Compensatory hue shift in simultaneous color contrast as a function of separation between inducing and test fields. *Journal of Experimental Psychology, 71*, 405–413.

Powell, I. (1981). Lenses for correcting chromatic aberration of the eye. *Applied Optics, 20*, 4152–4155.

Powell, M. J. D. (1964). An efficient method for finding the minimum of a function in several variables without calculating derivatives. *Computer Journal, 7*, 155–162.

Pugh, E. N. & Mollon, J. D. (1979). A theory of the Π_1 and Π_3 colour mechanisms of Stiles. *Vision Research, 19*, 293–312.

Schein, S. J. & Desimone, R. (1990). Spectral properties of V4 neurons in the macaque. *Journal of Neuroscience, 10*, 3370–3389.

Sclar, G., Lennie, P. & DePriest, D. D. (1989). Contrast adaptation in the striate cortex of macaque. *Vision Research, 29*, 747–755.

Shapley, R. & Victor, J. D. (1979). The contrast gain control of the cat retina. *Vision Research, 19*, 431–434.

Shevell, S. K., Holliday, I. & Whittle, P. (1992). Two separate neural mechanisms of brightness induction. *Vision Research, 32*, 2331–2340.

Simonet, P. & Campbell, M. C. W. (1990). The optical transverse chromatic aberration on the fovea of the human eye. *Vision Research, 30*, 187–206.

Singer, B. & D'Zmura, M. (1992). Color contrast gain control. *Optical Society of America 1992 Annual Meeting Technical Digest, 23*, 62.

Singer, B., Han, K.-H. & D'Zmura, M. (1993). Color selectivity in contrast gain control. *Investigative Ophthalmology and Visual Science, (Suppl.), 34*, 764.

Smith, V. C. & Pokorny, J. (1975). Spectral sensitivity of the foveal cone photopigments between 400 and 500 nm. *Vision Research, 15*, 161–171.

Solomon, J. A., Sperling, G. & Chubb, C. (1993). The lateral inhibition of perceived contrast is indifferent to on-center/off-center segregation, but specific to orientation. *Vision Research, 33*, 2671–2683.

Sperling, G. (1989). Three stages and two systems of visual processing. *Spatial Vision, 4*, 183–207.

Stiles, W. S. (1949). Increment thresholds and the mechanisms of colour vision. *Documenta Ophthalmologica, 3*, 138–163.

Thibos, L. N., Bradley, A., Still, D. L., Zhang, X. & Howarth, P. A. (1990). Theory and measurement of ocular chromatic aberration. *Vision Research, 30*, 33–49.

Tiplitz Blackwell, K. & Buchsbaum, G. (1988). The effect of spatial and chromatic parameters on chromatic induction. *Color Research and Application, 13*, 166–173.

Van Meeteren, A. (1974). Calculations on the optical modulation transfer function of the human eye for white light. *Optical Acta, 21*, 395–412.

Wald, G. & Griffin, D. R. (1947). The change in refractive power of the human eye in dim and bright light. *Journal of the Optical Society of America, 37*, 321–336.

Walraven, J. (1973). Spatial characteristics of chromatic induction; the segregation of lateral effects from straylight artifacts. *Vision Research, 13*, 1739–1753.

Wässle, H. & Heinrich, F. (1970). Untersuchungen zum Helligkeitskontrast. *Vision Research, 10*, 361–373.

Webster, M. A. & Mollon, J. D. (1991). Changes in colour appearance following post-receptoral adaptation. *Nature, 349*, 235–238.

Wesner, M. F. & Shevell, S. K. (1992). Color perception within a chromatic context: Changes in red/green equilibria caused by non-contiguous light. *Vision Research, 32*, 1623–1634.

Worthey, J. A. & Brill, M. H. (1986). Heuristic analysis of von Kries color constancy. *Journal of the Optical Society of America A, 3*, 1708–1712.

Wyszecki G. & Stiles, W. S. (1982). *Color science. Concepts and methods, quantitative data and formulas* (2nd edn). New York: Wiley.

Yund, E. W. & Armington, J. C. (1975). Color and brightness contrast effects as a function of spatial variables. *Vision Research, 15*, 917–929.

Zaidi, Q., Yoshimi, B., Flanigan, N. & Canova, A. (1992). Lateral interactions within color mechanisms in simultaneous induced contrast. *Vision Research, 32*, 1695–1707.

Zhang, X., Bradley, A. & Thibos, L. N. (1993). Experimental determination of the chromatic difference of magnification of the human eye and the location of the anterior nodal point. *Journal of the Optical Society of America A, 10*, 213–220.